Theoretical and Experimental Thermal Performance Analysis of Complex Thermal Storage Membrane Containing Bio-Based Phase-Change Material (PCM)

Jan Kosny, PhD
Member ASHRAE

Therese Stovall, PE
Member ASHRAE

Som Shrestha, PhD
Associate Member ASHRAE

David Yarbrough, PhD, PE
Member ASHRAE

ABSTRACT

A research team at Oak Ridge National Laboratory (ORNL) has been testing different configurations of PCM-enhanced building envelope components to be used in residential and commercial buildings. During 2009, a novel type of thermal storage membrane was evaluated for building envelope applications. Bio-based PCM was encapsulated between two layers of heavy-duty plastic film, forming a complex array of small PCM cells. Today, a large group of PCM products are packaged in such complex PCM containers or foils containing arrays of PCM pouches of different shapes and sizes. The transient characteristics of PCM-enhanced building envelope materials depend on the quality and amount of PCM, which is very often difficult to estimate because of the complex geometry of many PCM heat sinks. The only widely used small-scale analysis method to evaluate the dynamic characteristics of PCM-enhanced building products is the differential scanning calorimeter (DSC). Unfortunately, this method requires relatively uniform, and very small, specimens of the material. However, in numerous building thermal storage applications, PCM products are not uniformly distributed across the surface area, making the results of traditional DSC measurements unrealistic for these products. In addition, most of the PCM-enhanced building products contain blends of PCM with fire retardants and chemical stabilizers. This combination of nonuniform distribution and nonhomogenous composition makes it nearly impossible to select a representative small specimen suitable for DSC tests. Recognizing these DSC limitations, ORNL developed a new methodology for performing dynamic heat flow analysis of complex PCM-enhanced building materials. An experimental-analytical protocol to analyze the dynamic characteristics of PCM thermal storage makes use of larger specimens in a conventional heat flow meter apparatus, and combines these experimental measurements with three-dimensional (3D) finite-difference modeling and whole-building energy simulations. Based on these dynamic tests and modeling, ORNL researchers then developed a simplified one-dimensional (1D) model of the PCM-enhanced building component that can be easily used in whole-building simulations. This paper describes this experimental-analytical methodology as used in the analysis of an insulation assembly containing a complex array of PCM pouches. Based on the presented short example of whole-building energy analysis, this paper describes step by step how energy simulation results can be used for optimization of PCM-enhanced building envelopes. Limited results of whole-building energy simulations using the EnergyPlus program are presented, as well.

INTRODUCTION

Since the late 1980s, the ORNL research team has been working to evaluate different types of PCM-enhanced building insulation and board products, including dynamic thermal insulations blended with micro-encapsulated PCMs (Tomlinson et al. 1992: Kosny et al. 2006; Miller and Kosny 2007). In addition, several new products containing arrays of PCM micro-containers were laboratory and field tested. Most of these PCM-enhanced materials function as lightweight thermal-mass components of buildings. It is expected that dynamic envelope systems of this type will contribute to reducing energy use in buildings and to the development of "net-zero-energy" buildings through their ability to reduce energy consumption for space conditioning and peak loads.

Jan Kosny *was previously a senior research scientist at the Oak Ridge National Laboratory, Oak Ridge, TN, and is currently at the Fraunhofer Center for Sustainable Energy Systems (CSE), Cambridge, MA.* ***Therese Stovall***, ***Som Shrestha***, *and* ***David Yarbrough*** *are research scientists at the Oak Ridge National Laboratory, Oak Ridge, TN.*

© 2010 ASHRAE.

Other anticipated advantages of PCMs are improvement of occupant comfort, compatibility with traditional wood and steel framing technologies, and potential for application in retrofit projects. Previous studies (Salyer and Sircar 1989; Tomlinson et al. 1992; Feustel 1995; Kissock et al. 1998; Zhang et al. 2005; Kosny et al. 2007a, 2007b) have demonstrated that the use of PCMs in well-insulated buildings can reduce heating and cooling energy in US residential buildings by as much as 25% in locations with useful diurnal temperature variations.

PCM-enhanced interior sheathing based on *n*-octadecane has been considered in the past (Salyer and Sircar 1989; Tomlinson et al. 1992; Kissock et al. 1998), but concerns about flammability led the project team to pursue the development of ignition-resistant micro- and macro-encapsulated PCMs. In addition, in several ORNL projects, PCM was moved away from the interior sheathing. In a series of experiments carried out in a manufacturing environment, PCM was blended with fibrous insulations intended for use in walls and attics. As a result, the first two PCM-enhanced fiber insulations were ready for market introduction in the United States in 2009 (Kosny et al. 2009).

PCMs and other thermally massive materials are prominent in most plans for the advanced building envelope, and should be carefully characterized. No nationally accepted small-scale (in the order of 0.25 m or 0.82 ft) testing procedure is currently available to analyze the dynamic thermal characteristics of conventional thermal mass systems or PCM-enhanced materials. At the same time, data on these characteristics are required for whole-building simulations, energy analyses, and energy codes.

Figure 1 *Array of tested PCM cells packed in dense fiberglass insulation.*

The main goal of this work was the experimental and theoretical analysis of the energy performance of a relatively complex array of PCM cells, in this case comprising an insulation assembly (Figure 1). Numerous publications report obtaining the thermal characteristics of PCM materials using a differential scanning calorimeter (DSC).

In this project, a standard testing procedure using a heat flow meter apparatus (HFMA) was modified to allow dynamic testing. (Normally, the HFMA is used for steady-state thermal conductivity tests of horizontally homogenous materials as specified in *ASTM Standard C518, Standard Test Method for Steady-State Thermal Transmission Properties by Means of the Heat Flow Meter Apparatus*.) Dynamic HFMA testing was followed by finite-difference simulations. A detailed 3D computer model was developed to simulate the dynamic thermal ramp process carried out and monitored in the HFMA. In this computer model, the enthalpy data generated during the DSC tests were modified to represent the proportional weights of PCM and fire retardant in the PCM cells. Simplified 1D models were then developed based on the dynamic HFMA tests and 3D transient thermal simulations. One of these simplified 1D models was later used in whole-building energy simulations.

DESCRIPTION OF TESTED PCM TECHNOLOGY

In this project, an organic PCM was packed in plastic, as shown in Figure 1. The PCM product formed an assembly of 4.45 cm × 4.45 cm × 1.2 cm (1.75 in. × 1.75 in. × 0.47 in.) plastic cells containing PCM separated by 1.2 cm (0.47 in.) fiberglass strips. For testing purposes (and because the specimen had an irregular shape), the array of PCM cells was sandwiched between 1.9 cm (0.75 in.) thick dense, industrial-grade fiberglass on the top and 1.2 cm (0.47 in.) thick extruded polystyrene foam on the bottom, having thermal conductivities of 0.030 W/(m·K) and 0.039 W/(m·K) (0.017 Btu/h·ft·°F and 0.023 Btu/h·ft·°F), respectively.

First, researchers conducted a detailed analysis of the distribution of PCM in the individual cells. The cells, which contain fire retardant as well as PCM, were cut open, and the content was removed and weighed. The tested cells contained about 80 wt% of the organic PCM, with the balance being fire retardant, and about 20% of each PCM cell volume was filled with air. Researchers found that the PCM was not uniformly distributed among the individual plastic cells in these test samples (Figure 2). On average, there was about 11 g (0.024 lb) of PCM per cell, or about 176 g (0.388 lb) for the entire 30 cm × 30 cm (12 in. × 12 in.) test specimen. Assuming the total enthalpy of PCM was about 112 J/g (48.1 Btu/lb), the total heat storage capacity of the tested area was about 20 kJ (19 Btu).

SMALL-SCALE DSC TESTING OF PCM SAMPLES

The heat storage capacity of a PCM-enhanced product is a key indicator of its future dynamic thermal performance. For most common materials, a theoretical model of the material

with temperature-dependent specific heat can be used. The 1D heat transport equation for such a case is as follows:

$$\frac{\partial}{\partial t}(\rho h) = \frac{\partial}{\partial x}\left[\lambda \frac{\partial T}{\partial x}\right] \quad (1)$$

where t and x are time and distance, ρ and λ are material density and thermal conductivity, and h and T are enthalpy density and temperature.

The enthalpy derivative with respect to temperature, $\partial h/\partial T$, represents an effective heat capacity having phase-change energy as one of its components:

$$c_{eff} = \frac{\partial h}{\partial T} \quad (2)$$

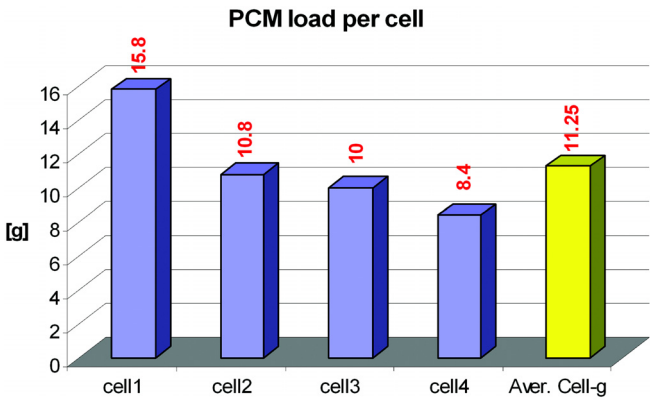

Figure 2 *Example of PCM load distribution.*

DSCs are commonly used for experimental analysis of phase-change energy in homogeneous materials. In this project, the thermal characteristics of chemically pure PCM were analyzed using a Seiko DSC220, which was programmed to heat from 0°C to 40°C (32°F to 104°F) and then to cool from 40°C to 0°C (104°F to 32°F). The heating/cooling rates were 0.3°C (0.54°F) and 1°C (1.8°F) per minute. Figure 3 shows the DSC thermogram for one of the tests with a heating/cooling rate of 0.3°C (0.54°F) per minute. The summarized DSC data for both tests are presented in Table 1.

DYNAMIC HFMA TESTING AND FINITE-DIFFERENCE THERMAL MODELING

A series of HFMA tests were performed to analyze the dynamic thermal characteristics of the PCM test specimen. The main purpose of this experimental exercise was to determine whether the enthalpy data received from DSC testing can be used to predict the energy performance of PCM-enhanced materials. Another question was whether the entire volume of PCM, distributed nonuniformly in the 30.5 cm × 30.5 cm (12 in. × 12 in.) insulation assembly, will work with the same effectiveness in the large-scale experiment in the HFMA as it did during the small-scale DSC testing.

Figure 4 shows the HFMA with the PCM-enhanced specimen used for the testing. (The picture shows the specimen supported by a thin composite plate, which was later replaced with a piece of 1.2 cm (0.47 in.) thick extruded polystyrene foam.) In this work, the HFMA experimental method was modified to allow dynamic testing of PCM-enhanced materials. During the heat flow meter test, the total specimen thickness of approximately 6.4 cm (2.5 in.) was brought to a uniform temperature of 15.5°C (59.9°F) by setting both plates

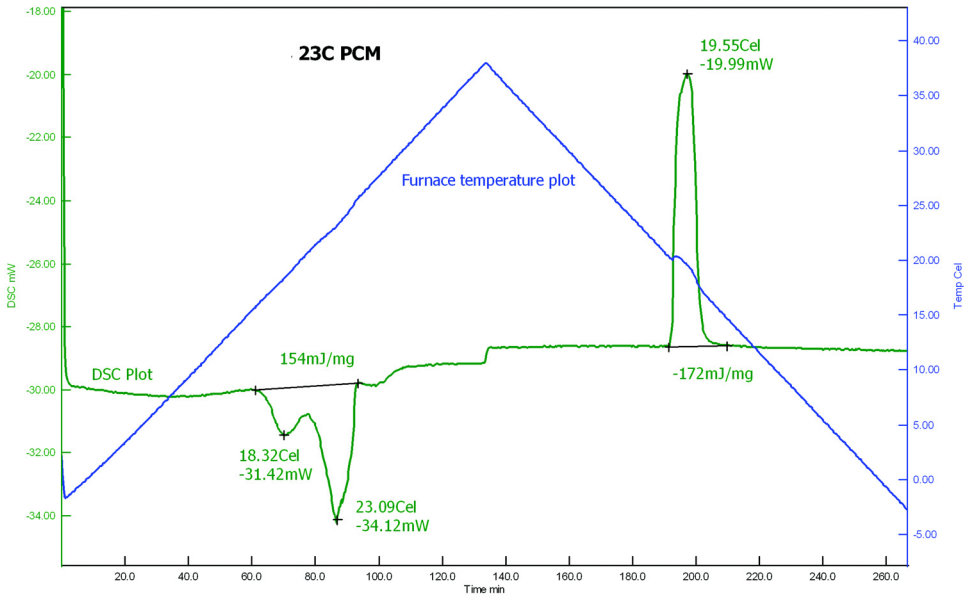

Figure 3 *Figure 3. DSC test data for heating/cooling rate of 0.3°C per minute.*

Table 1. DSC Results for PCM Labeled 23°C (73.4°F)

Heating and Cooling Rates, °C/minute (°F/minute)	Melt Energy, J/g (Btu/lb)	Freeze Energy, J/g (Btu/lb)	Melt Temperature, °C (°F)*	Freeze temperature, °C (°F)
0.3 (0.54)	160 (68.8)	172 (74.0)	18/23 (64.4/73.4)	20 (68)
1.0 (1.8)	157 (67.5)	173 (74.4)	19/26 (66.2/78.8)	19 (66.2) (Rep B)

*The DSC enthalpy curve showed two peaks during the melting process; both temperatures are listed here.

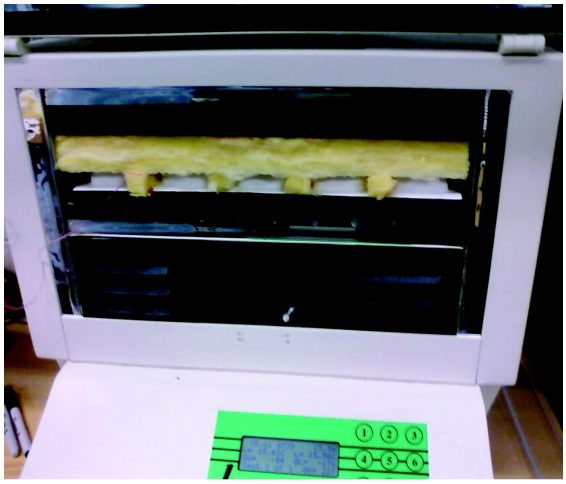

Figure 4 *Heat flow meter apparatus used to test PCM-enhanced materials.*

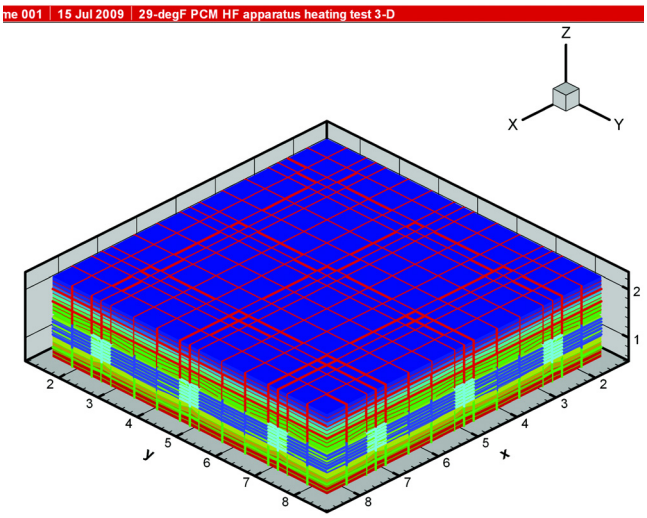

Figure 5 *Three-dimensional computer model used in dynamic simulations.*

in the HFMA at the same temperature. At time zero, the temperature of the bottom plate of the HFMA was changed to 43°C (109.4°F), with a resulting heat flux toward the test specimen. The heat flux and HFMA plate temperatures were monitored continuously. It took approximately 3 minutes for the bottom plate to reach the desired temperature. The experiment was finished after heat flows on both HFMA plates were stabilized at constant levels.

In addition to dynamic HFMA testing, a series of finite-difference simulations was performed using Heating 7.2 (Childs 1993). A detailed 3D computer model was developed for the same PCM-enhanced specimen that was tested. Figure 5 illustrates the complexity of the finite-difference model.

Both 3D and 1D computer models used modified apparent enthalpy curves, which were based on results of the DSC testing. Critical information from the DSC testing used in the models included peak melting temperature, total enthalpy, temperature range for the melting process, and the general shape of the enthalpy curve. As shown in Figure 3, the enthalpy profile for the 23°C (73.4°F) PCM is relatively complex, with two peaks during the melting process and a single peak during the freezing process. In Table 1, the total enthalpy is listed as 157 J/g to 173 J/g (67.5 Btu/lb to 74.4 Btu/lb) and peak temperature as 18°C to 26°C (64.4°F to 78.8°F). For modeling purposes, it was assumed that the shape of the enthalpy curve was relatively flat (one peak each for melting and freezing) and that the total enthalpy value was 160 J/g (68.8 Btu/lb). In addition, the effect of the fire retardant was included by reducing the total enthalpy value by 20%.

Next, based on a comparison between the experimental data and the results from a series of transient 3D simulations, it was found that not all the PCM worked (melted or froze) during the thermal ramp process. Previous ORNL research on similarly packed PCM blends with different materials has shown that 10% to 30% of the PCM may not melt or freeze. Results of a detailed analysis of temperature fields across the tested specimen revealed that this behavior is likely due to complex three-dimensional effects in corners of the PCM pouches (Kosny et al. 2009). A similar phenomenon has been also reported by other laboratories (Mehling and Cabeza 2008; Günther et al. 2009). In case of microencapsulated PCMs, this effect can be caused by relatively common mechanical damage or leakage of microcapsules. This effect can be also a result of greater-than-desired amounts of admixtures being blended with the PCM, and from the variable purity of some PCMs. Therefore, the enthalpy value was reduced by extra 10% (giving total 30% reduction). As a result, 112 J/g (48.1 Btu/lb) was used in the final numerical model. With a total of about 176 g (0.388 lb) of PCM used in the entire test

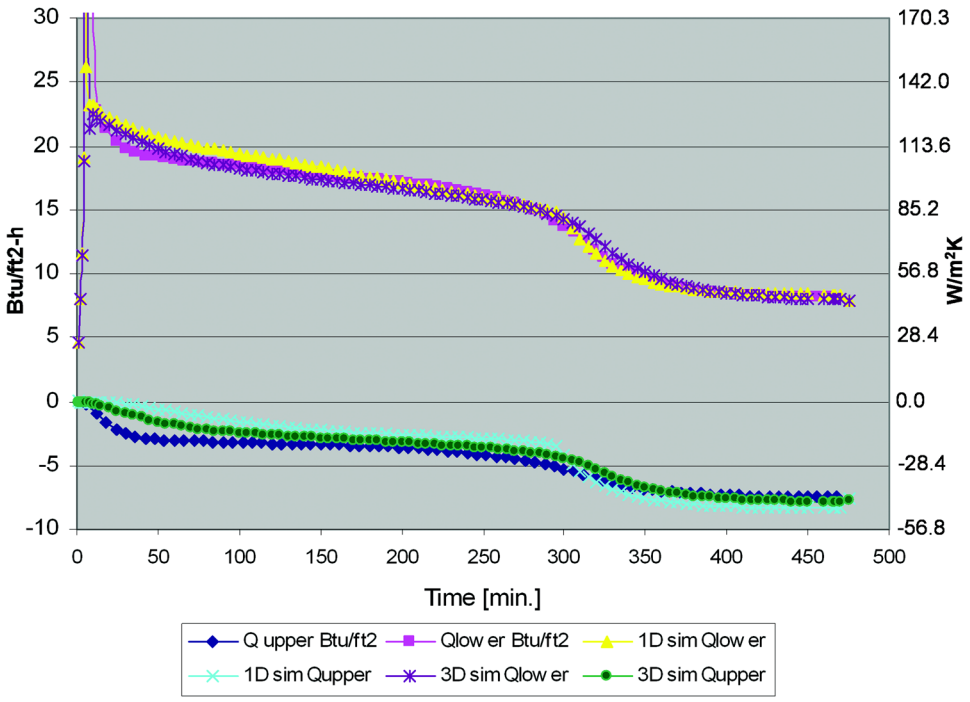

Figure 6 *Comparisons of simulated and tested heat flows on both HFMA plates for the 23°C PCM.*

specimen, the total latent heat capacity of the tested specimen was then about 20 kJ (19 Btu). A comparison of HFMA test results and the 3D and 1D simulations is shown in Figure 6, where the heat flows from both the top and bottom plates of the HFMA are in good agreement with the model when the adjusted enthalpy curve is used.

In order to enable whole-building simulations, a simplified 1D computer model was developed using the equivalent wall procedure from Kossecka and Kosny (1997) and ASHRAE (2002) Research Project RP-1145. Most whole-building energy computational models have 1D algorithms for transient thermal simulations. ASHRAE (2002) provides a detailed description of a theoretical procedure that can be used to convert 3D thermal models into simplified 1D models. This process can generate a family of different solutions (several different 1D models) having similar transient characteristics.

Energy stored during the HFMA experiment was computed as well. Heat flows for each of the HFMA plates were integrated over time based on the test data recorded during the dynamic HFMA experiment. The difference between the integrated top and bottom plate heat flow was 20.1 kJ (19.1 Btu). In a similar way, the simulated heat flows were integrated over the time. The stored energy was 21.0 kJ (19.9 Btu) for the 3D model and 20.9 kJ (19.9 Btu) for the 1D model. This yielded 4.5% and 4.1% differences, respectively, when compared to the test results.

EXAMPLE OF NUMERICAL WHOLE-BUILDING ENERGY ANALYSIS USING ENERGYPLUS WHOLE-BUILDING ENERGY SIMULATIONS

In this section, an example of the application of whole-building energy simulation is presented in order to describe different theoretical methods that can be used for optimization of PCM technologies for walls and roofs. A series of whole-building energy simulations was performed using a previously developed simplified 1D model of a PCM-enhanced assembly. The energy performance of a residential building with and without PCM-enhanced assembly in exterior wall was studied using the building energy simulation tool EnergyPlus 4.0. The building considered for the study was a 16.8 m × 8.4 m (55 ft × 27.5 ft) single-story ranch house with three bedrooms, one living room, and an attic. Figure 7 shows the building used for the study.

The conventional conduction transfer function (CTF) heat balance algorithm used by EnergyPlus assumes constant thermal properties of all construction materials. Therefore, this method cannot be used to simulate any building with a PCM-enhanced envelope assembly. Hence, for both building models, the model without PCM (case 1), and the model with PCM-enhanced exterior walls (case 2), the conduction finite difference (CondFD) heat balance algorithm was used to calculate heat transfer across the building envelope.

Simulated exterior walls of the building without PCM were composed of the exterior layer, the air gap with

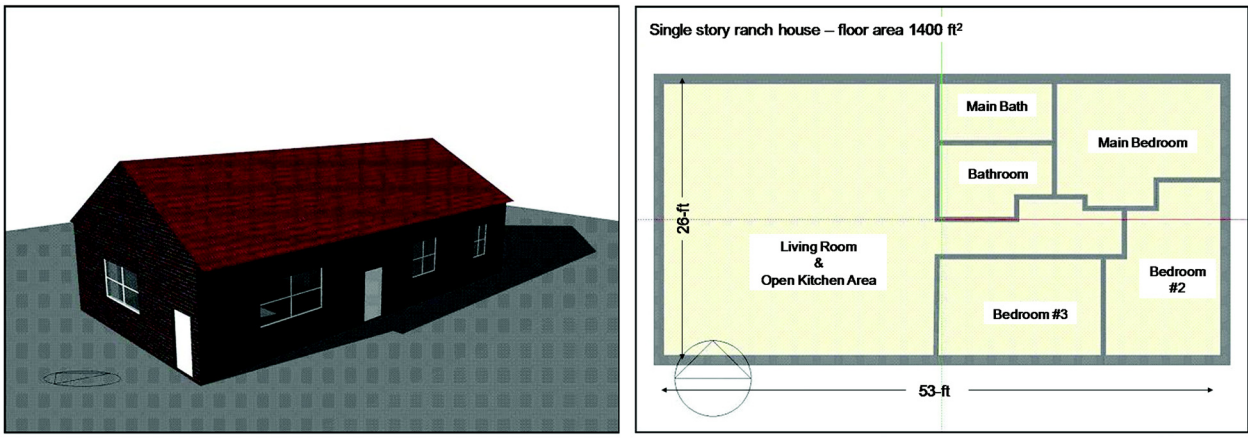

Figure 7 *Building model used for the study: 16.8 m × 8.4 m (55 ft × 27.5 ft) single-story ranch house.*

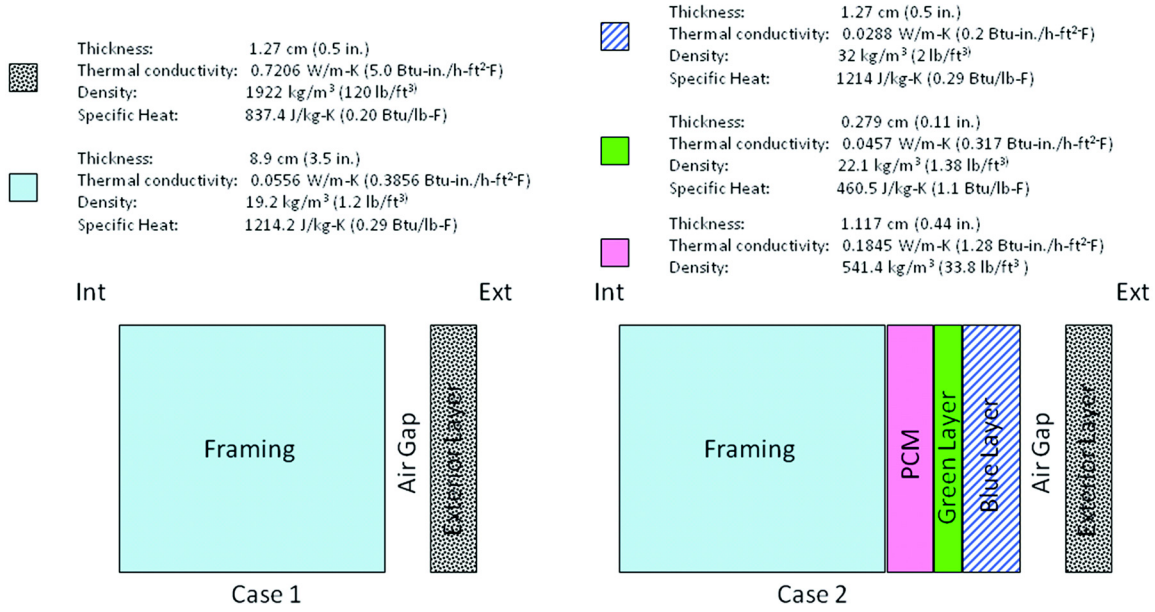

Figure 8 *Composition of exterior walls and thermal properties of each layer.*

0.33 (m^2·K)/W (1.88 ft^2·°F·h/Btu) thermal resistance, and the framing layer (representing a conventionally insulated 2 × 4 stud wall), as shown on Figure 8. Exterior walls of the building with the PCM-enhanced assembly have three additional layers of fictitious materials: the blue layer, green layer, and PCM layer, situated between the air gap and the framing layer. This combination of three layers, produced by the theoretical procedure developed by Kossecka and Kosny for ASHRAE RP-1145 (ASHRAE 2002), represents a simplified one-dimensional model of these complex PCM pouches. In this fictitious 1D model, the material physical characteristics do not represent a real material (Kossecka and Kosny 1997; Kosny et al. 2009). Figure 8 shows the composition of the exterior walls for case 1 and case 2 and the thermal properties of each layer. The enthalpy-temperature relationship of the phase change material layer is presented in Figure 9.

In the building model, a direct-expansion type cooling coil was used for cooling and a combination of heat pump with electric heater was used for heating. Minimum outdoor dry-bulb temperature was set at –8°C (17.6°F) for the heat pump. Building heating and cooling temperatures were set at 22°C (71.6°F) and 26°C (78.8°F), respectively. EnergyPlus simulations of both building models were performed using an Atlanta weather file, and the results were used to calculate seasonal

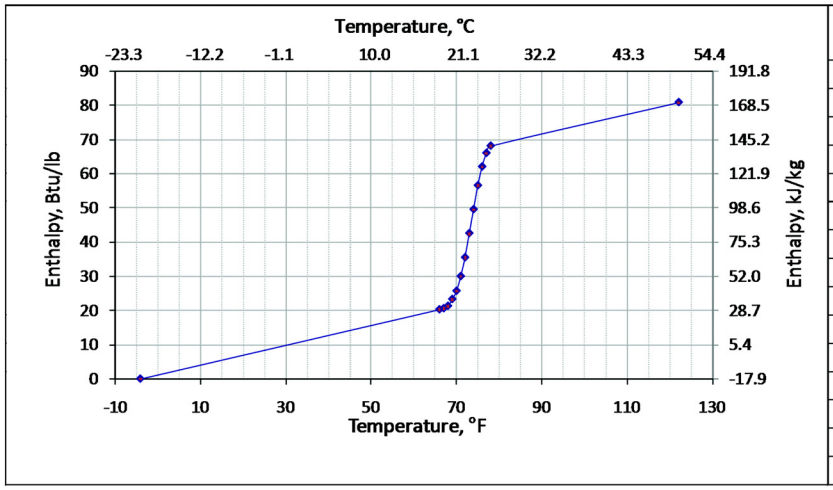

Temperature, °C (°F)	Enthalpy, kJ/kg (Btu/lb)
-20.0 (-4)	-17.88 (0)
18.9 (66)	29.34 (20.3)
19.4 (67)	30.11 (20.63)
20.0 (68)	31.74 (21.33)
20.6 (69)	36.39 (23.33)
21.1 (70)	41.98 (25.73)
21.7 (71)	51.98 (30.03)
22.2 (72)	64.77 (35.53)
22.8 (73)	81.06 (42.53)
23.3 (74)	97.34 (49.53)
23.9 (75)	113.6 (56.53)
24.4 (76)	126.4 (62.03)
25.0 (77)	135.7 (66.03)
25.6 (78)	140.6 (68.13)
50.0 (122)	170.3 (80.89)

Figure 9 *Enthalpy-temperature relationship of the phase-change material used in energy analysis.*

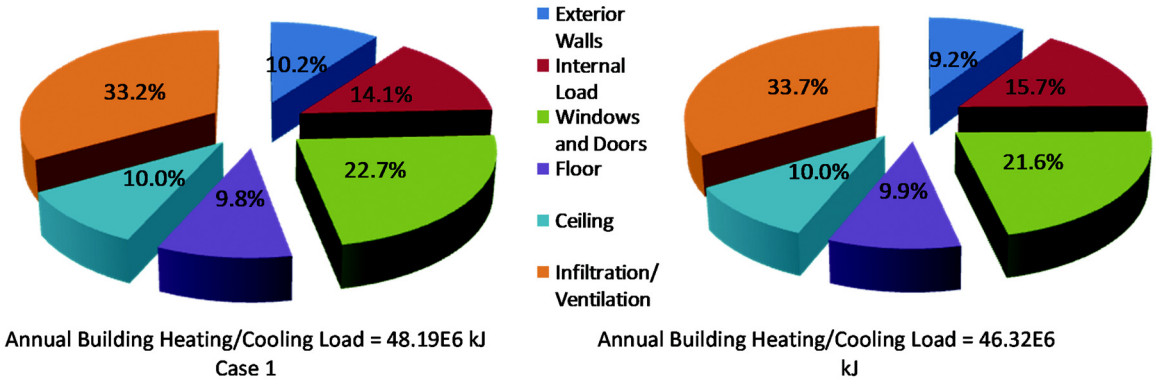

Figure 10 *Load distribution to each source for the case 1 and case 2 buildings.*

Table 2. Comparisons between Performances of the Building with and without PCM

Heating / Cooling Load	Exterior Wall		% Change from Case 1
	Case 1	Case 2	
Annual heating/cooling load associated with exterior wall heat transfer, kJ	4,907,363	4,246,543	–13.5%
Annual exterior wall load, as % of annual whole-building heating/cooling load	10.2%	9.2%	–9.8%

and annual heating/cooling load associated with heat flow through exterior walls, windows/doors, floor, ceiling, infiltration/ventilation, and internal load.

Exterior-wall heat gains and heat losses for heating and cooling periods were calculated for each hour to determine the net heat gains during the cooling period and the net heat loss during the heating period. Annual heating/cooling load associated with heat flow through exterior walls is the sum of the net heat gain during the cooling period and the net heat loss during the heating period. A similar approach was used to calculate whole-building loads. Annual heating/cooling load distributions for case 1 and case 2 are shown in Figure 10. The comparisons between energy performances of the case 1 (non-PCM) and case 2 (PCM) buildings are presented in Table 2. This preliminary EnergyPlus simulation showed that, for the building configuration studied, PCM with the effective phase-change heat storage density of 112 kJ/kg (48.1 Btu/lb) applied in all exterior walls has the potential to save about 13.5% of the heating/cooling loads associated with the exterior walls in that climate.

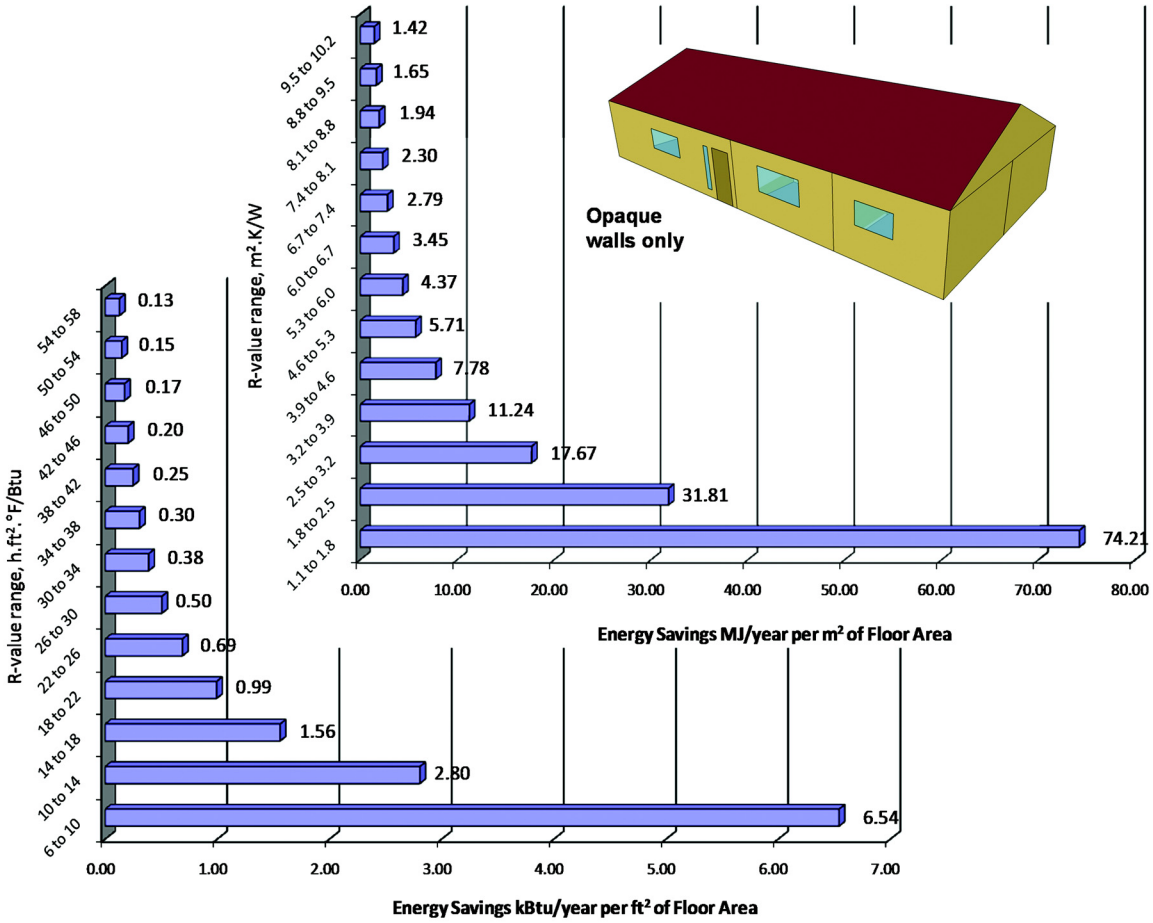

Figure 11 *Diminishing returns for added wall insulation simulated for Atlanta weather.*

Since addition of PCM to the building envelope components can be expensive, a detailed study should always be performed in order to determine whether it would be cost-effective to use a PCM-enhanced assembly on a specific wall, attic, or roof. Diminishing energy savings returns can be observed on Figure 11, which depicts potential heating/cooling load savings associated with addition of R_{SI}-0.7 (R-4) insulation on the exterior walls for a single-story residential building located at Atlanta. It is noticeable that addition of the same insulation R-value to the better-insulated walls generates significantly lower energy savings compared to the same R-value addition to the poorly insulated walls. This fact should be always considered when an application of PCM is evaluated against conventional insulation.

In order to further optimize PCM application, an additional analysis can be performed to determine how many times the PCM was melted/solidified during specific months of the year. Climatic data for the month of July in Atlanta were selected to simulate the phase change temperature profiles. Figure 12 shows the temperature profiles across the south-facing wall containing PCM. Two solid horizontal lines show the phase change temperature range (including subcooling effect) for the PCM used in this study. Apparently, the PCM never fully solidified during July. Looking at Figure 11, one might be tempted to increase the phase-change temperature to get more benefit from PCM. However, it should be taken into consideration that the scenario for other months and other walls can be significantly different than the PCM temperature profile shown in Figure 12. An application of PCM with higher melting point may improve energy performance during July, but it may also reduce a number of active days during spring and fall months. In order to optimize the phase-change temperature for a given climate a series of simulations with various phase-change temperatures must be carried out.

It is also important to remember that PCM should be always considered as energy-saving enabling technology that is used in association with other thermal control systems (like, for example, thermal insulation or radiant barriers). Very often, an addition of PCM components may increase the R-value of building envelopes. That is why both conduction heat transfer and thermal mass effects should be carefully separated. The heating/cooling load saving potential a of PCM-

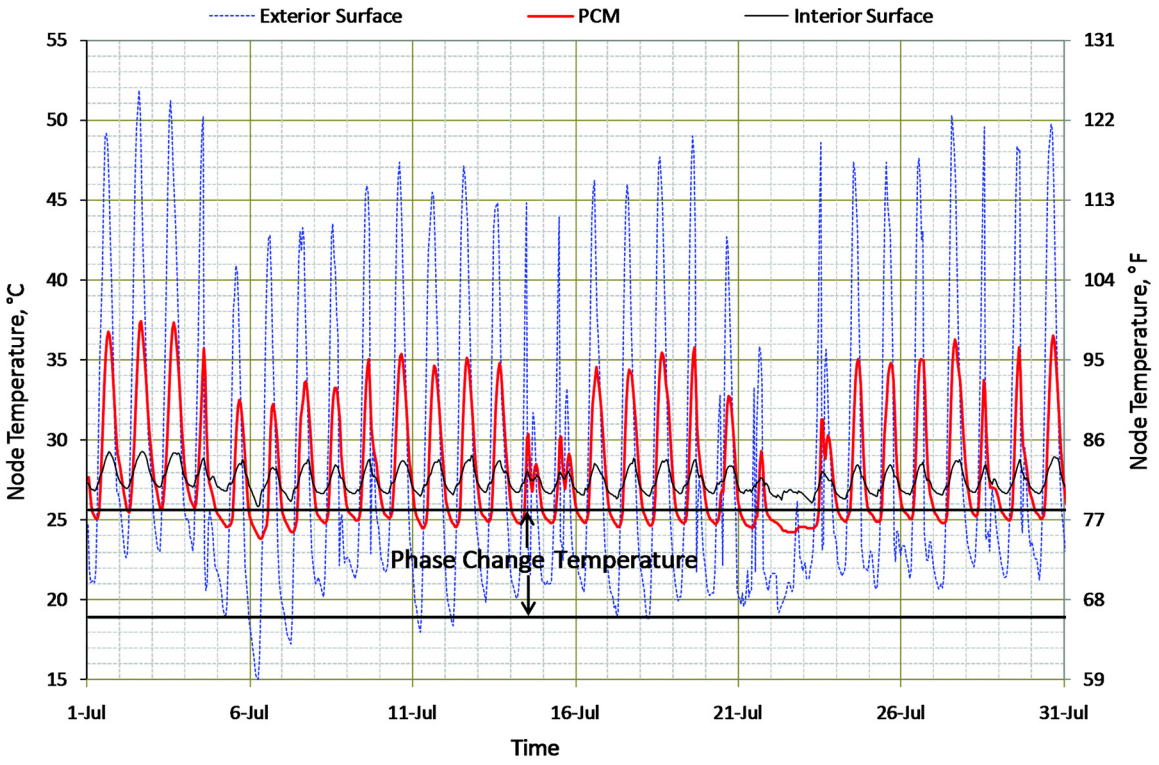

Figure 12 *Simulated temperature profiles across the south-facing wall for July.*

enhanced assembly applied on exterior walls shown in Table 2 can be subdivided into two parts: (1) savings due to added insulation, and (2) savings due to heat storage potential of PCM. While ignoring phase-change enthalpy of PCM, thermal resistance of added PCM-enhanced assembly is equivalent to R_{SI}-0.6 (R-3.2), as depicted in Figure 8. Simulation of the case 1 building with R_{SI}-0.6 (R-3.2) insulation added between the air gap and framing showed annual heating/cooling load associated with wall heat transfer as 4,728,4 kJ. In that light, a total 13.5% heating/cooling load savings associated with an addition of the PCM-enhanced layers to the exterior walls can be divided into 3.65% load saving achieved due to added insulation and 9.85% load saving achieved due to thermal performance of PCM.

In yet another study, the dynamic R-value equivalent procedure developed by Kosny et al. (2001) for energy performance analysis of thermal mass systems was used. In order to calculate the effect of the PCM-enhanced assembly applied on the residential attic floor, a series of whole-building energy simulations were performed on a single-story ranch house located in Atlanta. Two configurations of the attic floor insulation were considered for the study:

- Conventional attic floor insulation within a range of R_{SI}-6.7 (R-38) to R_{SI}-17.3 (R-98) considered with R-value increments of R_{SI}-2.2 (R-12)
- Attic floor with PCM-enhanced assembly installed on top of the R_{SI}-6.7 (R-38) insulation. Table 3 shows the annual heating/cooling load associated with heat transfer through the ceiling for each case. Figure 13 presents the data for ceiling without PCM-enhanced assembly.

Without considering the thermal storage capability of PCM due to phase change, the equivalent thermal resistance of the ceiling with PCM-enhanced assembly on top of R_{SI}-6.7 (R-38) insulation is R_{SI}-7.3 (R-41.2). Interpolation using the curve-fit equation is shown on Figure 13 for data presented in Table 3. It gives an annual heating/cooling load generated by the attic with R_{SI}-7.3 (R-41.2) insulation as 5,333,609 kJ. For the PCM-enhanced assembly installed on top of the R_{SI}-6.7 (R-38) insulation, the annual heating/cooling load is 4,588,337 kJ, which is 14% less than the load with R_{SI}-7.3 (R-41.2) conventional attic floor insulation. Next, the dynamic R-value equivalent was computed based on results from the parametric energy simulations. As shown on Figure 13, conventional attic floor insulation of approximately R_{SI}-10.3 (R-58.3) would be required to achieve the same level of heating/cooling loads (associated with the ceiling heat transfer) as in case of the PCM-enhanced R_{SI}-6.7 (R-38) insulation for this location. In other words, an additional R_{SI}-3.7 (R-22.1) of conventional insulation would be required on top of the R_{SI}-6.7 (R-38) conventional insulation in order to generate the same annual loads as in case of the R_{SI}-6.7 (R-38) PCM-

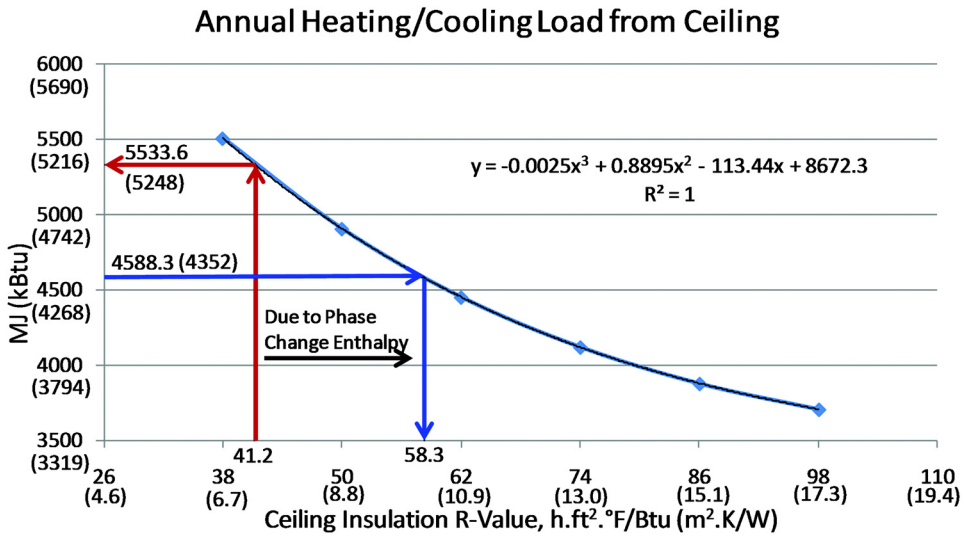

Figure 13 *Comparisons of attic-generated annual heating/cooling loads.*

Table 3. Annual Heating Cooling Load from Ceiling

Ceiling Configuration	Annual Heating/Cooling Load Associated with Ceiling Heat Transfer, kJ
Ceiling with R-38 insulation	5,506,583
Ceiling with R-50 insulation	4,906,446
Ceiling with R-62 insulation	4,452,029
Ceiling with R-74 insulation	4,120,299
Ceiling with R-86 insulation	3,878,320
Ceiling with R-98 insulation	3,706,999
Ceiling with PCM-enhanced assembly on top of R-38 insulation	4,588,337

enhanced insulation for this climate. This would require about 15 cm (6 in.) of extra space.

SUMMARY

A novel type of thermal storage membrane was evaluated for building envelope applications. Bio-based PCM was encapsulated between two layers of heavy-duty plastic film, forming a complex array of small PCM cells. This paper discusses a novel experimental-analytical methodology that can be used in the analysis of an insulation assembly containing a complex array of PCM pouches. Based on the short example of whole-building energy analysis presented, this paper describes step by step how energy simulation results can be used to optimize PCM-enhanced building envelopes.

A heat flow meter apparatus (HFMA) designed for steady-state thermal conductivity measurements was used to observe the performance of PCM imbedded in an insulation assembly. The HFMA test results and the DSC data were combined with a 3D finite difference model to determine the effective heat capacity of the system. The procedure that was developed permits an evaluation of the heat storage capacity of a PCM-enhanced building component and its response to changing temperatures. In order to enable whole-building simulations, a simplified 1D computer model was developed using the equivalent wall procedure.

An example of energy performance analysis based on results of whole-building energy simulations of a 141.12 m^2 (1512.5 ft^2) residential building located in Atlanta with and without PCM on exterior walls and attic was presented. Energy simulations were performed using EnergyPlus building energy simulation software. The results of preliminary energy simulations showed about a 10% reduction in annual wall-generated heating and cooling loads for the building with PCM-enhanced exterior walls in this location. An application of PCM in exterior walls was compared against an application of a similar wall using conventional insulations of equivalent R-value. The dynamic R-value equivalent procedure was used for analysis of the PCM-enhanced attic insulation. In order to calculate the effect of the PCM-enhanced assembly applied on the residential attic floor, a series of whole-building energy simulations was performed on a single-story ranch house located in Atlanta. Results of the limited energy modeling demonstrated that, in Atlanta, a conventional attic floor insulation of approximately R_{SI}-10.3 (R-58.3) would be required to achieve the same level of heating/cooling loads as in case of the PCM-enhanced R_{SI}-6.7 (R-38) insulation. For the considered case of the R_{SI}-6.7 (R-38) PCM-enhanced insulation results of the whole-building energy simulations demonstrated a potential for about 14% reduction of the attic-generated annual loads comparing to the conventional R_{SI}-6.7 (R-38) insulation.

The bio-based PCM samples used for the heat flow meter apparatus tests described in this work were early prototypes. The manufacturer's current products use enhanced formulations with better energy management properties and are manufactured to higher tolerances. The results presented in this paper can be only considered as an example of the energy performance analysis of PCM-enhanced building envelope technologies. The PCM system used in this analysis was optimized neither for the wall nor for the attic applications.

REFERENCES

ASHRAE. 2002. *Modeling two- and three-dimensional heat transfer through composite wall and roof assemblies in hourly simulation programs*. Report, Research Project RP-1145. Atlanta, GA: American Society of Heating, Refrigerating and Air-Conditioning Engineers, Inc.

ASTM. 2006. *ASTM Standard C518, Standard Test Method for Steady-State Thermal Transmission Properties by Means of the Heat Flow Meter Apparatus*. West Conshohocken, PA: American Society of Testing and Materials.

Childs, K.W. 1993. *Heating 7.2 user's manual*. Oak Ridge National Laboratory Report ORNL/TM-12262.

Feustel, H.E. 1995. *Simplified numerical description of latent storage characteristics for phase change wallboard*. Berkeley: Lawrence Berkeley National Laboratory, Indoor Environmental Program, Energy and Environment Division.

Günther, E., S. Hiebler, H. Mehling, and R. Redlich. 2009. Enthalpy of phase change materials as a function of temperature: Required accuracy and suitable measurement methods. *International Journal of Thermophysics* 30(4).

Kissock, J.K, M.J. Hannig, and T.I. Whitney. 1998. Testing and simulation of phase change wallboard for thermal storage in buildings. *Proceedings of 1998 International Solar Energy Conference*, Albuquerque. Sponsored by American Society of Mechanical Engineers, New York.

Kosny, J., D. Gawin, and A. Desjarlais. 2001. Energy benefits of application of massive walls in residential buildings. *DOE, ASHRAE, ORNL Conference—Thermal Envelopes VIII*, Clearwater, FL.

Kosny, J., D. Yarbrough, and K. Wilkes. 2006. PCM-enhanced cellulose insulation: thermal mass in lightweight fibers. *International Energy Agency and Department of Energy Ecostock 2006 Conference*, Stockton University.

Kosny, J., D. Yarbrough, T.W. Petrie, and A. Syed. 2007a. Performance of thermal insulation containing microencapsulated phase change material. *2007 International Thermal Conductivity Conference*, Birmingham, AL.

Kosny, J., D. Yarbrough, W. Miller, T. Petrie, P. Childs, and A. Syed. 2007b. Thermal performance of PCM-enhanced building envelope systems. *DOE, ASHRAE, ORNL Conference—Thermal Envelopes X*, Clearwater, FL.

Kosny, J., T. Stovall, and D. Yarbrough. 2009. Dynamic heat flow measurements to study the distribution of phase-change material in an insulation matrix. *Proceedings of the 2009 International Thermal Conductivity Conference (ITCC) and the International Thermal Expansion Symposium (ITES)*, Pittsburgh, PA.

Kossecka, E. and J. Kosny. 1997. Equivalent wall as a dynamic model of the complex thermal structure. *Journal of Thermal Insulation and Building Envelopes* 20:249–68.

Mehling, H. and L.F. Cabeza. 2008. *Heat and cold storage with PCM: An up to date introduction into basics and applications*. Springer.

Miller, W.A., and J. Kosny. 2007. Next generation roofs and attics for residential homes. *Proceedings of the 2007 ACEEE Summer Studies on Energy Efficiency*, Pebble Beach, CA.

Salyer, I. and A. Sircar. 1989. Development of PCM wallboard for heating and cooling of residential buildings. *Thermal Energy Storage Research Activities Review, US Department of Energy*, New Orleans, pp. 97–123.

Tomlinson, J., C. Jotshi, and D. Goswami. 1992. Solar thermal energy storage in phase change materials. *Proceedings of Solar '92: The American Solar Energy Society Annual Conference*, Cocoa Beach, FL, pp. 174–79.

Zhang, M., M.A. Medina, and J. King. 2005. Development of a thermally enhanced frame wall with phase-change materials for on-peak air conditioning demand reduction and energy savings in residential buildings. *International Journal of Energy Research* 29(9):795–809.